Investigation of Buckling Phenomenon Induced by Growth of Vertebral Bodies Using a Mechanical Spine Model*

Ryu SASAOKA**, Hideyuki AZEGAMI***, Shunji MURACHI****, Junzoh KITOH†, Yoshito ISHIDA††, Noriaki KAWAKAMI†††, Mitsunori MAKINO†††† and Yukihiro MATSUYAMA†††††

A hypothesis that idiopathic scoliosis is a buckling phenomenon of the fourth or sixth mode, which is the second or third lateral bending mode, induced by the growth of vertebral bodies was presented in a previous paper by the authors using numerical simulations with a finite-element model of the spine. This paper presents experimental proof of the buckling phenomenon using mechanical spine models constructed with the geometrical data of the finite-element model used in a previous work. Using three spine mechanical models with different materials at intervertebral joints, the change in the natural vibration eigenvalue of the second lateral bending mode with the growth of vertebral bodies was measured by experimental modal analysis. From the result, it was observed that natural vibration eigenvalue decreased with the growth of vertebral bodies. Since the increase in primary factor inducing the buckling phenomenon decreases natural vibration eigenvalue, the obtained result confirms the buckling hypothesis.

Key Words: Biomechanics, Idiopathic Scoliosis, Growth, Buckling, Mechanical Spine Model, Experimental Modal Analysis

1. Introduction

Idiopathic scoliosis is known as a spinal irregularity with lateral curvatures without any marked abnormality of vertebrae or associated musculoskeletal conditions. Since almost all cases of this disease appear during adolescence, especially during growth spurt, it has been recognized that growth is associated with the etiology of idiopathic scoliosis in some ways.

On the etiology of idiopathic scoliosis from a mechanical point of view, the authors have presented a hypothesis that idiopathic scoliosis is a buckling phenomenon of the fourth or sixth mode, which is the second or third lateral bending mode, induced by the growth of vertebral bodies using numerical simulations with a finite-element model of the spine[1),(2)]. To confirm the existence of the buckling phenomenon, attempts to observe this phenomenon using mechanical models were made in our previous studies[3),(4)]. In our first study[3)], although a straight spine column model consisting of vertebral bodies and intervertebral disks with a rectangular cross-section equipped

* Received 23rd May, 2003 (No. 03-4063)

** Doctoral Course of Graduate School of Mechanical and Structural System Engineering, Toyohashi University of Technology, 1-1 Hibarigaoka, Tempaku-cho, Toyohashi, Aichi 441-8580, Japan. E-mail: sasaoka@az.mech.tut.ac.jp

*** Department of Complex Systems Science, Graduate School of Information Science, Nagoya University, Furo-cho, Chigusa-ku, Nagoya, Aichi 464-8601, Japan. E-mail: azegami@is.nagoya-u,ac.jp

**** Japanese Red Cross Aichi Junior College of Nursing, 3-35 Michishita-cho, Nakamura-ku, Nagoya, Aichi 453-0046, Japan

† Emer. Prof. of Nagoya University School of Medicine, 65 Tsurumai-cho, Showa-ku, Nagoya, Aichi 466-8550, Japan. E-mail: jkitoh@med.nagoya-u.ac.jp

†† Ishida Orthopaedic Surgery, 90-1 Sadamatsu, Takao, Huyou-cho, Tanba County, Aichi 480-0102, Japan. E-mail: iy01-ioc@na.rim.or.jp

††† Orthopaedic Surgery, Meijyo Hospital, 1-3-1 Sannomaru, Naka-ku, Nagoya, Aichi 460-0001, Japan. E-mail: noriaki@pop12.odn.ne.jp

†††† Orthopaedic Surgery, Toyota Memorial Hospital, 1-1 Heiwa-cho, Toyota, Aichi 471-0821, Japan. E-mail: m_makino@mail.toyota.co.jp

††††† Spine service, School of Medicine, Nagoya University, 65 Tsurumai-cho, Showa-ku, Nagoya, Aichi 466-8550, Japan. E-mail: spine-yu@med.nagoya-u.ac.jp

with a growth mechanism that uses screws was constructed, a buckling phenomenon was not observed without an angular constraint at the top of the column. Considering the importance of the physiological curvature of the spine, in the succeeding study[4], a mechanical spine model was constructed using geometrical data of the finite-element model used in numerical simulations and examined to observe the buckling phenomenon by means of vibration testing; however, to recognize the buckling phenomenon, slight compression load at the top of the spine column was required. In this study, the insufficiency of the stiffness of intervertebral joints was pointed out.

The objective of this paper is to show the existence of the buckling phenomenon induced by the growth of vertebral bodies purely from a mechanical point of view for better understanding of the buckling hypothesis for determining the mechanical etiology of idiopathic scoliosis. Based on previous studies, in this study, three mechanical spine models were carefully reconstructed in stiffness and posture using different materials for intervertebral joints. These models were used to show experimental proof of the buckling phenomenon by measuring the change in natural vibration eigenvalue, the natural vibration mode of which is similar to the second lateral bending buckling mode, with the growth of vertebral bodies. To measure natural vibration eigenvalue, experimental modal analysis was employed. The theoretical background of the change in natural vibration eigenvalue with the growth of vertebral bodies is demonstrated in this study.

2. Mechanical Spine Models

To confirm the existence of the buckling phenomenon that were confirmed by numerical analysis using a finite-element spine model in previous studies[2],[5],[6], mechanical spine models that have the same geometrical configuration as the numerical spine model were constructed. The finite-element spine model had been constructed using a solid modeler (I-DEAS Master series version 2.1, SDRC) with commercial data of three-dimensional configuration of the spine (Viewpoint Premier, catalog numbers of VP2886 and VP3611, Viewpoint Co., Ltd)[5].

The photographs of the mechanical spine model constructed in this study are shown in Fig. 1. The model consists of vertebrae, intervertebral disks and intervertebral joints from the first cervical vertebra to the top of the sacrum.

The vertebrae and intervertebral disks were fabricated by casting. Their template models were made using a three-dimensional milling machine (Modela MDX-15, Roland DG Co., Ltd.) with chemical wood

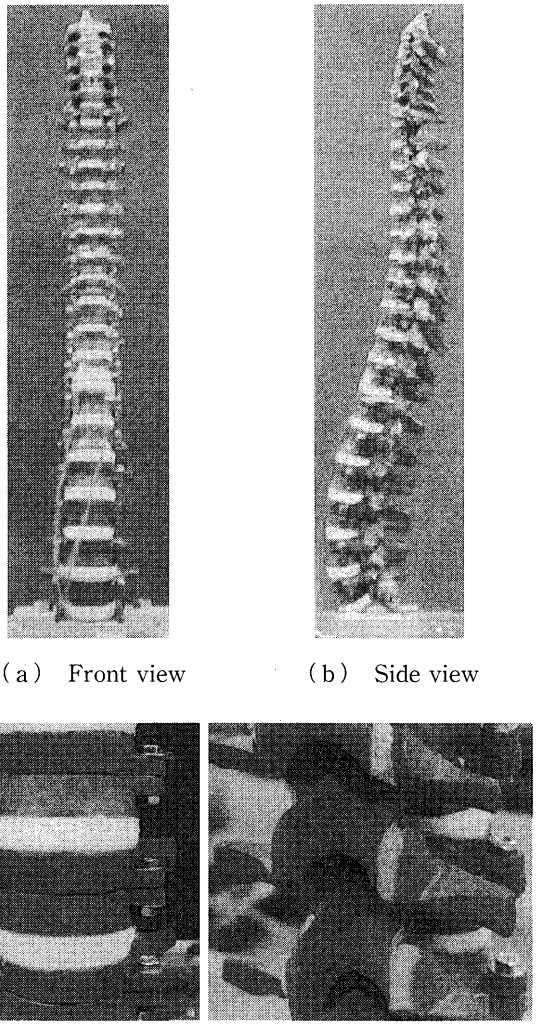

(a) Front view (b) Side view

(c) Magnified front view (d) Magnified rear view

Fig. 1 Mechanical spine model constructed in this study

(Sunmodule MH, Tagiyashouten Corporation) using geometrical data of the finite-element model used in numerical simulations[5]. The molds of the template models were made of silicone RTV rubber (Shinetsu KE-14, Shin-Etsu Chemical Co., Ltd.). The vertebrae were molded out of nonfoaming hard polyurethane resin (HEI-CAST, Heisen Yoko Co., Ltd.). The intervertebral disks were molded out of silicone RTV rubber (Shinetsu KE-17, Shin-Etsu Chemical Co., Ltd.) and glued to the vertebrae with silicone filler (Bath-caulk, Cemedine Co., Ltd.). The intervertebral joints were formed by filling gaps between the vertebrae with the following materials.

A) Silicone filler (Bath-Caulk, Cemedine Co., Ltd.)

B) Modified silicone polymer (Silex, Konishi Co., Ltd.)

C) Room-temperature setting-color urethane rubber (ADAPT 80 L, Nissin Resin Co., Ltd.)

In this paper, let the mechanical spine models with the three materials at the intervertebral joints be called

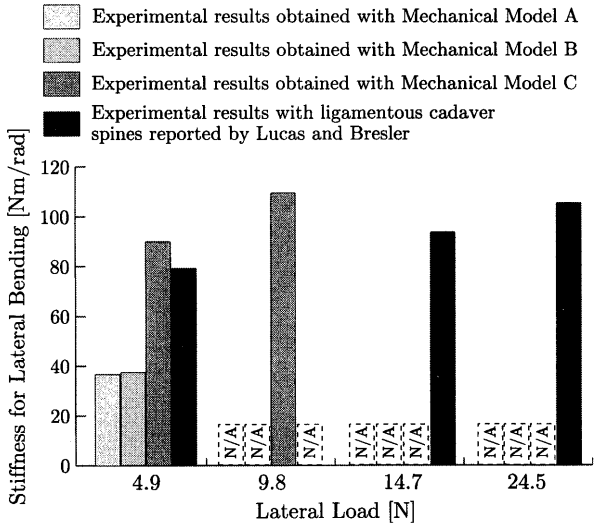

Fig. 2 Comparison of lateral bending stiffness between experimental results reported by Lucas and Bresler[7] and experimental results obtained with mechanical spine models in this study

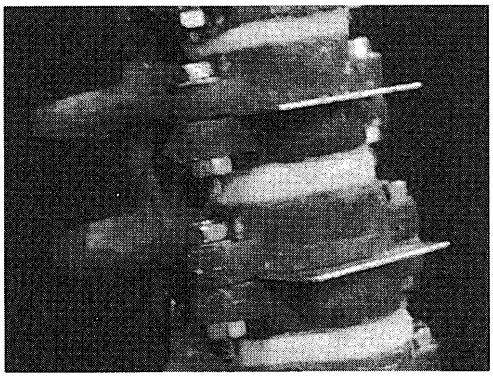

Fig. 3 Growth of vertebrae with plates of various thicknesses

Models A, B and C, respectively. In the process of constructing the mechanical spine models, jigs were fabricated using a fused deposition modeling rapid prototyping system (Genisys Xs, Stratasys Inc.) and used for improving the precision of the position of the vertebrae and the gaps between the vertebrae.

Comparing the mechanical spine model with the finite-element model, it was assumed that a thoracic cage is omitted, the nucleus pulposus is made of the same material with anulus fibrosus and vertebrae are made of a homogeneous material. Young's modulus of the intervertebral disks was 2.5 MPa (data from the manufacturer) that agrees with Young's modulus of the anulus fibrosus in the finite-element model. Young's modulus of the intervertebral joints of Model C was 9 MPa (data from the manufacturer) compared with 7.5 MPa for the finite-element model. Although there were no data from the manufacturers for Young's moduli of the intervertebral joints of Models A and B, it was decided that they were obviously smaller than that of Model C through examination by touch. Lateral bending tests on the mechanical spine models were carried out. Figure 2 shows the comparison of stiffness for lateral bending with experimental results obtained using ligamentous cadaver spines devoid of musculature by Lucas and Bresler[7]. From the result, it was determined that Model C had the same lateral bending stiffness as cadaver spines and Models A and B had a smaller lateral bending stiffness than cadaver spines.

The vertebrae were lengthened by inserting plates of various thicknesses into the vertebrae divided into upper and lower parts and fastening the plates with bolts through holes in the flanges on the upper and lower parts of the vertebrae as shown in Fig. 3. Although the growth mechanism inserting plates is different from the mechanism underlying the actual growth of the vertebrae and may cause different stress distributions in intervertebral joints and disks, it is considered that global deformation with the growth of vertebrae was simulated. As in the case of numerical simulations, considering the results obtained by Dickson et al.[8] and the authors[5],[6], the fourth thoracic vertebra up to the tenth thoracic vertebra were lengthened under the fixed sacrum and the freely supported top of the spine column. Although the buckling phenomenon was analyzed as a bifurcation point on the initial deformation of the growth by linear buckling analysis in numerical simulations, the buckling phenomenon or state immediately before the buckling phenomenon occurred in the process of fastening bolts in the mechanical models.

3. Natural Vibrations of Continuum with Initial Deformation

Stable lateral bending deformations like the second lateral bending buckling mode were observed during the process fastening bolts and drawing the fifth cervical vertebra up to the normal position. However, it was judged that to accurately measure the change in displacement or stress during the process of fastening bolts and drawing the cervical vertebra up to the normal position is difficult. Thus, we measured the change in natural frequency, the natural vibration mode of which is similar to the second lateral bending buckling mode with respect to the growth of vertebral bodies based on the theoretical relation that if the natural vibration mode is similar to the buckling mode, natural frequency corresponding to the natural vibration mode decreases.

The theoretical background of the above-mentioned decrease is as follows. Assuming that the growth is given by bulk strain as in previous studies[1],[5], the variational form of the eigenvalue

equation for the linear elastic continuum defined in domain $\Omega \in \mathbb{R}^3$ with respect to a small displacement is

$$a(\boldsymbol{u}^{(0)}, \boldsymbol{v}^{(0)}) = a_\varepsilon(\boldsymbol{\varepsilon}^B, \boldsymbol{v}^{(0)}) \quad \boldsymbol{u}^{(0)} \in U \quad \forall \boldsymbol{v}^{(0)} \in U \tag{1}$$

$$a(\boldsymbol{u}^b, \boldsymbol{v}^b) = -\zeta d(\boldsymbol{u}^{(0)}, \boldsymbol{u}^b, \boldsymbol{v}^b) \quad \boldsymbol{u}^b \in U \quad \forall \boldsymbol{v}^b \in U, \tag{2}$$

where bilinear forms $a(\cdot, \cdot)$, $a_\varepsilon(\cdot, \cdot)$, and the trilinear form $d(\cdot, \cdot, \cdot)$ are defined by

$$a(\boldsymbol{u}^b, \boldsymbol{v}^b) \equiv \int_\Omega C_{ijkl} u^b_{k,l} v^b_{i,j} dx \tag{3}$$

$$a_\varepsilon(\boldsymbol{\varepsilon}^B, \boldsymbol{v}^b) \equiv \int_\Omega C_{ijkl} \varepsilon^B_{kl} v^b_{i,j} dx \tag{4}$$

$$d(\boldsymbol{u}^{(0)}, \boldsymbol{u}^b, \boldsymbol{v}^b) \equiv \int_\Omega C_{ijkl} u^{(0)}_{k,l} u^b_{m,i} v^b_{m,j} dx \tag{5}$$

and U denotes the admissible set for the displacement satisfying boundary conditions. Equation (1) denotes the variational form of elastic deformation for determining prebuckling displacement $\boldsymbol{u}^{(0)}(=\boldsymbol{u}^{(0)}(\boldsymbol{x})=\{u_i^{(0)}(\boldsymbol{x})\}_{i=1}^3 : \Omega \ni \boldsymbol{x} \mapsto \boldsymbol{u}^{(0)} \in \mathbb{R}^3)$ due to the generation of bulk strain $\boldsymbol{\varepsilon}^B(=\boldsymbol{\varepsilon}^B(\boldsymbol{x})=\{\varepsilon^B_{ij}(\boldsymbol{x})\}_{i,j=1}^3 : \Omega \ni \boldsymbol{x} \mapsto \boldsymbol{\varepsilon}^B \in \mathbb{R}^{3\times3})$ using virtual displacement $\boldsymbol{v}^{(0)}$. Equation (2) denotes variational form of the eigenvalue equation for the buckling loading factor $\zeta \in \mathbb{R}$ and buckling mode $\boldsymbol{u}^b$ using the virtual mode $\boldsymbol{v}^b$. The tensor $\{C_{i,j,k,l}\}_{i,j,k,l=1}^3 : \Omega \mapsto \mathbb{R}^{3\times3\times3\times3}$ denotes stiffness. In this study, a tensor notation with subscripts, the Einstein summation convention and the gradient notation $(\cdot)_{,i} = \partial(\cdot)/\partial x_i (\{x_i\}_{i=1}^3 \in \mathbb{R}^3)$ are used.

The variational form of the equation of motion for the time-dependent displacement $\boldsymbol{u}(=\boldsymbol{u}(\boldsymbol{x}, t)=\{u_i(\boldsymbol{x}, t)\}_{i=1}^3 : \Omega \times \mathbb{R} \ni (\boldsymbol{x}, t) \mapsto \boldsymbol{u} \in \mathbb{R}^3)$ of the continuum with initial deformation $\boldsymbol{u}^{(0)}$ by generating initial bulk strain $\boldsymbol{\varepsilon}^B$ is[9]

$$a(\boldsymbol{u}, \boldsymbol{v}) + d(\boldsymbol{u}^{(0)}, \boldsymbol{u}, \boldsymbol{v}) = -b(\ddot{\boldsymbol{u}}, \boldsymbol{v}) \quad \boldsymbol{u} \in U_t \quad \forall \boldsymbol{v} \in U_t, \tag{6}$$

where bilinear form $b(\cdot, \cdot)$ is

$$b(\boldsymbol{u}, \boldsymbol{v}) \equiv \int_\Omega \rho u_i v_i dx, \tag{7}$$

and U_t is the admissible set for the time-dependent displacement satisfying boundary conditions. ρ denotes density. In this paper, the dot notation for the time differential $\dot{(\cdot)} = \partial(\cdot)/\partial t$ is used. Based on Eq. (6), the variational form of the eigenvalue equation for the r-th natural vibration eigenvalue $\lambda^{[r]}$ defined by the square of the r-th natural frequency, and the natural vibration mode $\boldsymbol{u}^{[r]}$ is

$$a(\boldsymbol{u}^{[r]}, \boldsymbol{v}) + d(\boldsymbol{u}^{(0)}, \boldsymbol{u}^{[r]}, \boldsymbol{v}) = \lambda^{[r]} b(\boldsymbol{u}^{[r]}, \boldsymbol{v}) \quad \boldsymbol{u}^{[r]} \in U \quad \forall \boldsymbol{v} \in U \tag{8}$$

Considering Eq. (2) in Eq. (8),

$$a(\boldsymbol{u}^{[r]} - \boldsymbol{u}^b, \boldsymbol{v}) + d(\boldsymbol{u}^{(0)}, \boldsymbol{u}^{[r]} - \zeta \boldsymbol{u}^b, \boldsymbol{v}) = \lambda^{[r]} b(\boldsymbol{u}^{[r]}, \boldsymbol{v}) \quad \boldsymbol{u}^{[r]}, \boldsymbol{u}^b \in U \quad \forall \boldsymbol{v} \in U \tag{9}$$

If $\boldsymbol{u}^{[r]}$ is assumed as the mode normalized by $b(\boldsymbol{u}^{[r]}, \boldsymbol{u}^{[r]})=1$ and is used for $\boldsymbol{v}$,

$$\lambda^{[r]} = a(\boldsymbol{u}^{[r]} - \boldsymbol{u}^b, \boldsymbol{u}^{[r]}) + d(\boldsymbol{u}^{(0)}, \boldsymbol{u}^{[r]} - \zeta \boldsymbol{u}^b, \boldsymbol{u}^{[r]}) \tag{10}$$

If $\boldsymbol{u}^b$ is normalized by $b(\boldsymbol{u}^b, \boldsymbol{u}^b)=1$ and agrees with $\boldsymbol{u}^{[r]}$, the first term on the right-hand side of Eq. (10) becomes zero. In this case, r-th natural vibration eigenvalue $\lambda^{[r]}$, which is a positive real number when $\boldsymbol{u}^{(0)}=\boldsymbol{0}$, decreases with increasing initial deformation $\boldsymbol{u}^{(0)}$ and approaches zero at $\zeta=1$. A typical case where $\boldsymbol{u}^{[r]}$ agrees with $\boldsymbol{u}^b$ can be found for beam structures under axial force[10].

The spine model is closely analogous to beam structures. Therefore, if the buckling occurs and boundary conditions are selected to generate the r-th natural vibration mode close to the buckling mode, the existence of the buckling phenomenon can be confirmed by measuring the decrease in r-th natural eigenvalue $\lambda^{[r]}$ with respect to the increase in initial deformation.

4. Experimental Modal Analysis

To measure the decrease in natural eigenvalue, experimental modal analysis was employed. In this study, the fifth cervical vertebra was excited in the lateral direction with harmonic force using an electrodynamic shaker (511-A, Emic Co., Ltd.) fixed on the side of the fifth cervical vertebra as shown in Fig. 4(a). Force was measured with a piezoelectric force transducer (PF-31, Rion Co., Ltd.) screwed to the fifth cervical vertebra via a driving rod from the shaker. Response to the excitation was measured at seventeen points using six accelerometers (PV-90B, Rion Co., Ltd.) that were fixed on the mechanical model with wax. Charge amplifiers (VP-14A, Rion Co., Ltd.) were used to amplify output signals.

Natural frequencies and natural vibration modes from the first mode to the fourth mode were analyzed with an experimental modal analysis system (VIBRANT-GEN, Marubeni Solutions Co., Ltd.) using seventeen transfer functions at the measurement points of acceleration. Figure 4(b) shows the

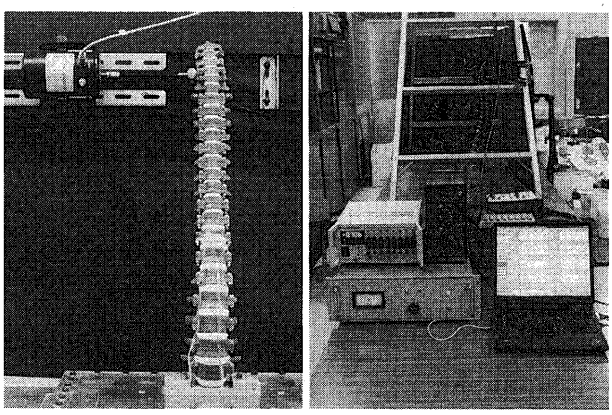

(a) Excitation system (b) Modal analysis system

Fig. 4 Schematics of experimental modal analysis system

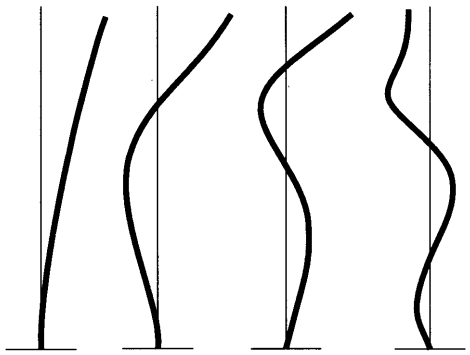

(a) Mode 1 (b) Mode 2 (c) Mode 3 (d) Mode 4

Fig. 5 Natural vibration modes

schematic of the analysis system. Figure 5 shows the results for the natural vibration modes. From these results, it is judged that the second natural vibration mode is in good agreement with the second lateral bending buckling mode.

Based on the agreement of the second natural vibration mode with the second lateral bending buckling mode, measurement was focused on the change in the second natural frequency. For accuracy in measurement, the frequency response function of bending strain was measured using two strain gauges (KFP-5-120-C1-65 L2M2R, Kyowa Electronic Instruments Co., Ltd.) stuck on both sides of the front surface of the eleventh thoracic vertebra by taking the difference between the output signals from the two gauges. A bridge box (DB-120T-8, Kyowa Electric Instruments Co., Ltd.) and dynamic strain amplifiers (MCD-8A, DPE-71A, DPM-72A, Kyowa Electric Instruments Co., Ltd.) were used for the measurement of bending strain. The signals of the force and bending strain were captured on a personal computer via an A-D converter (Multichannel Data Station DS-2000 Series, Ono Sokki Co., Ltd.) and calculated to obtain the frequency response function using an FFT (Fast Fourier Transform) analyzer (CAT-System DS-0241M, Ono Sokki Co., Ltd.) installed on a personal computer.

Concerning the influence of the mass of the plates used for the growth of the vertebrae, it was confirmed that the difference in frequency response function between the cases of putting the plates on the front surface and removing them was negligible.

5. Result

The changes in natural vibration eigenvalue with respect to the growth of vertebral bodies which are given by the sum of the thicknesses of the plates inserted into the vertebral bodies is shown in Fig. 6. From the result, the natural vibration eigenvalues of models B and C decreased with an increase in the extent of growth. However, no change in the eigenvalue was observed for model A.

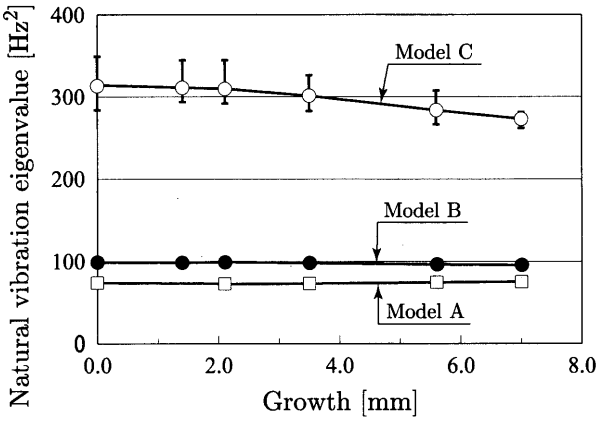

Fig. 6 Change in the second natural vibration eigenvalues with growth of vertebral bodies

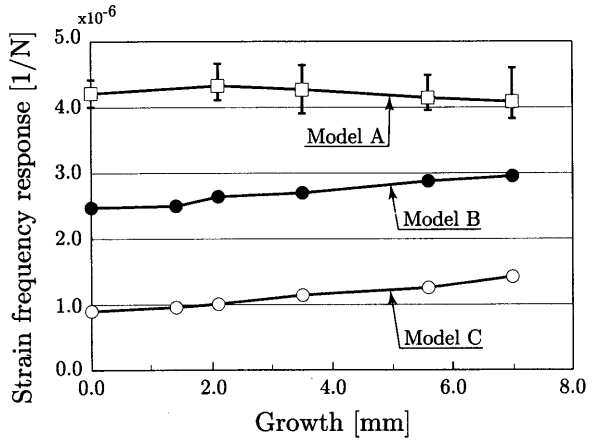

Fig. 7 Change in the magnitude of the strain frequency response functions at the second natural frequency with respect to growth of vertebral bodies

For determining the index of stiffness for the mechanical spine models, the change in the magnitude of the strain frequency response function at the second natural frequency with the growth of vertebral bodies was estimated. Figure 7 shows the result. As in the case of the natural vibration eigenvalues, the magnitudes of the strain frequency response functions of model B and C increased with increase in the extent of growth. However, no change in the magnitude of the strain frequency response function was observed for model A.

6. Discussion

As predicted in Section 3, the second natural vibration eigenvalue decreased with the growth of vertebral bodies for Models B and C, although the decrease was slight for Model B. For Model A, however, no marked changes were observed. The obvious difference of Model A with Models B and C is in terms of lateral bending stiffness, as shown in Fig.

2. Considering that the difference in lateral bending stiffness originated from the difference in material at intervertebral joints, it can be presumed that the resistance of the intervertebral joint is crucial for generating the second lateral bending buckling mode.

The amount of decrease in natural vibration eigenvalue with the growth of vertebral bodies in Fig. 6 was smaller than the theoretical expectation even for Model C. One of the main reasons for this can be considered as follows. Equation (10) was obtained on the assumption that the prebuckling displacement $\boldsymbol{u}^{(0)}$ is conservative or does not vary its direction following an increase in bulk strain $\boldsymbol{\varepsilon}^{B}$. However, in the present spine model, it is considered that the direction of $\boldsymbol{u}^{(0)}$ varied following the growth of vertebrae owing to the insertion of the plates. That a follower force can increase eigenvalues $\lambda^{[r]}$ has been reported previously[9]. The influence of nonconservativeness should be investigated in future studies. Another possibility that can be considered is the insufficient adhesion at intervertebral joints and disks. This insufficiency is considered to decrease the resistance that generates the buckling phenomenon.

In comparison with the numerical simulation in which the second lateral bending buckling mode occurred at 1.7 mm of growth of the vertebral bodies from the fourth thoracic vertebra to the tenth thoracic vertebra[1),2)], the use of Models B and C showed a tendency to decrease the second natural vibration eigenvalue from 1.5 mm of growth in Fig. 6. Although counting of the thoracic cages was performed in the finite-element spine model, the critical growths for Models B and C remained the same as that obtained by the numerical simulation.

As a characteristic that could not be accurately checked by numerical simulation, the stability of the second lateral bending buckling mode could be checked in this study. As described in the beginning of Section 3, the second lateral bending deformations observed in the process of fastening bolts and drawing the fifth cervical vertebra up to the normal position were stable. Even during the vibration testing, the mechanical spine models were stable.

7. Conclusion

In this paper, we presented experimental proof of the buckling hypothesis with respect to idiopathic scoliosis based on the theoretical relation that if the natural vibration mode is similar to the buckling mode, natural frequency decreases. Three mechanical spine models were constructed using three different materials at intervertebral joints. With these models, the change in the second natural vibration eigenvalue was measured by experimental modal analysis. The obtained result showing a decrease in the second natural vibration eigenvalue with the growth of vertebral bodies is confirms of the buckling hypothesis.

References

(1) Azegami, H., Murachi, S., Kitoh, J., Ishida, Y., Kawakami, N. and Makino, M., Etiology of Idiopathic Scoliosis: Computational Study, Clinical Orthopaedics and Related Research, No. 357 (1998), pp. 229-236.

(2) Takeuchi, K., Azegami, H., Sasaoka, R., Murachi, S., Kitoh, J., Ishida, Y., Kawakami, N., Goto, M., Makino, M. and Matsuyama, Y., Numerical Simulation on Etiology of Idiopathic Scoliosis: Modal Investigation. Spinal Deformity, The Journal of Japanese Scoliosis Society, (in Japanese), Vol. 16, No. 1 (2001), pp. 11-16.

(3) Azegami, H., Murachi, S., Kitoh, J., Ishida, Y., Kawakami, N. and Makino, M., An Experiment with a Mechanical Model on the Etiology of Idiopathic Scoliosis. Spinal Deformity, The Journal of Japanese Scoliosis Society, (in Japanese), Vol. 13, No. 1 (1998), pp. 29-32.

(4) Sasaoka, R., Takeuchi, K., Azegami, H., Murachi, S., Kitoh, J., Ishida, Y., Kawakami, N., Makino, M., Matsuyama, Y., Goto, M., Inoh, H. and Yoshihara, H., An Experiment with a Mechanical Model on the Etiology of Idiopathic Scoliosis: Examination with Precise Spine Model. Spinal Deformity, The Journal of Japanese Scoliosis Society, (in Japanese), Vol. 17, No. 1 (2002), pp. 18-22.

(5) Takeuchi, K., Azegami, H., Murachi, S., Kitoh, J., Ishida, Y., Kawakami, N. and Makino, M., Study on Treatment with Respect to Idiopathic Scoliosis: Sensitivity Analysis Based on Buckling Theory, JSME Int. J., Ser. C, Vol. 44, No. 4 (2001), pp. 1059-1064.

(6) Takeuchi, K., Azegami, H., Murachi, S., Kitoh, J., Ishida, Y., Kawakami, N. and Makino, M., Computational Study on the Etiology of Idiopathic Scoliosis: Buckling Hypothesis Induced by Bone Modeling against Gravity, Transactions of JSCES, (in Japanese), Vol. 4 (2002), pp. 153-160, (Paper No. 20020006 published Feb. 8, 2002).

(7) Lucas, D.B. and Bresler, B., Stability of the Ligamentous Spine, Biomechanics Laboratory Rpt. 40, Univ. of California, (1961).

(8) Dickson, R.A., Lawton, J.O., Archer, I.A. and Butt, W.P., The Pathogenesis of Idiopathic Scoliosis (Biplanar Spinal Asymmetry), J. Bone and Joint Surg., Vol. 66B (1984), pp. 8-15.

(9) Bolotin, V.V., The Dynamic Stability of Elastic Systems, (1964), Holden-Day, San Francisco.

(10) Kobayashi, S., Shindougaku, (in Japanese), (1994), Maruzen.